Purnomo, Budi Joko ; Pichler, Thomas

Geothermal systems on the island of Java, Indonesia

Journal Article as: peer-reviewed accepted version (Postprint)

DOI of this document*(secondary publication): https://doi.org/10.26092/elib/3222

Publication date of this document: 15/08/2024

* for better findability or for reliable citation

Recommended Citation (primary publication/Version of Record) incl. DOI:

Budi Joko Purnomo, Thomas Pichler, Geothermal systems on the island of Java, Indonesia, Journal of Volcanology and Geothermal Research, Volume 285, 2014, Pages 47-59, ISSN 0377-0273, https://doi.org/10.1016/j.jvolgeores.2014.08.004.

Geothermal systems on the island of Java, Indonesia

Budi Joko Purnomo [a,b,*], Thomas Pichler [a]

[a] Geochemistry & Hydrogeology, Department of Geosciences, University of Bremen, Germany
[b] Geological Agency of Indonesia, Bandung, Indonesia

Keywords:
Java
Volcano-hosted and fault-hosted geothermal systems
Geochemistry
^{2}H and ^{18}O isotope

1. Introduction

At least 62 geothermal fields with the potential for exploitation are present on the island of Java (Setijadji, 2010). Following Alam et al. (2010) geothermal fields can be divided into volcano-hosted and fault-hosted geothermal systems based on their geologic association. The former is a geothermal system related to a volcanic complex and the latter is a geothermal system located in a fault zone. To date, seven volcano-hosted geothermal fields were developed and five of them produce electricity. Fault-hosted geothermal fields were not developed and are rarely explored, due to the assumption of insufficient energy. However, considering the geology of Java, a volcanic (magmatic) influence on the fault-hosted geothermal systems is likely.

* Corresponding author at: Geochemistry & Hydrogeology, Department of Geosciences, University of Bremen, P.O. Box 33 04 40, 28334 Bremen, Germany. Tel.: +49 421 218 65119.

E-mail address: purnomo@uni-bremen.de (B.J. Purnomo).

In other volcanic arcs around the world, fault-hosted geothermal fields which are located close to volcanic areas indicate a heating of deep circulated meteoric water, e.g., in the Liquiñe-Ofqui fault zone of Chile and in the Southern Apennines of Italy (Alam et al., 2010; Italiano et al., 2010). Using a trend of B enrichment, Alam et al. (2010) suggested for the Liquiñe-Ofqui fault zone (a) heating of meteoric water in fault-zone hosted geothermal systems and (b) condensation of volcanic steam in volcano-hosted geothermal systems. However, the authors did not indicate the heat source of the fault-hosted geothermal system. Arehart et al. (2003) identified a magmatic heat source for the Steamboat geothermal system (Nevada, USA), based on trace metal and gas data. Historically this geothermal system was considered as an extensional geothermal type with anomalous heat flow as the heat source (Wisian et al., 1999). Anomalous heat flow in the Alpine fault, New Zealand, for example, is considered to be caused by uplift and erosion (Allis and Shi, 1995; Shi et al., 1996).

Here physicochemical processes, fluid sources and reservoir temperature of volcano and fault-hosted geothermal systems on Java were examined, using chemical and isotope (^2H and ^{18}O) data. The data indicated a magmatic influence on the fault-hosted geothermal systems, and thus a hidden energy potential for some of the fault-hosted geothermal systems on Java.

2. Geological setting

Java, an island in the Indonesian archipelago is a part of a long volcanic arc that extends from Sumatera to Nusa Tenggara (Fig. 1). The volcanic arc is due to subduction of the Indo-Australian plate beneath the Eurasian plate, with a rate of about 6 to 7 cm/a (Hamilton, 1979; Simandjuntak and Barber, 1996). The subduction started in the middle Paleogene (Hall, 2002) and produced the east–west trending Southern Mountain volcanic arc (Soeria-Atmadja et al., 1994). Later, in the magmatic periods of the Neogene and the Quaternary, additional volcanic arcs were formed to the north, also trending from east to west (Van Bemellen, 1949; Hamilton, 1979). The older rocks (Tertiary) are andesitic, while the younger (Quarternary) rocks are more alkaline (Soeria-Atmadja et al., 1994). Clements et al. (2009) noted that subduction caused lifting and erosion in the southern part of the island, as indicated by the exposure of Cretaceous basement.

The tectonic setting of Java is dominated by four main faults, namely the E–W backarc-thrust of Barabis–Kendeng, the NE–SW strike-slip fault of Cimandiri, the SE–NW Citandui fault in West Java and the NE–SW Central Java Fault (Hoffmann-Rothe et al., 2001). These faults were generated since the Neogene by compressional forces (Simandjuntak and Barber, 1996; Hall, 2002). The Cimandiri fault is an active fault with a slip rate of about 6 to 10 mm/a (Setijadji, 2010; Sarsito et al., 2011). The Citandui and the Central Java faults are a pair of major strike-slip faults (wrench faults) that formed the geological features of Central Java and caused a northward shift of the Quaternary volcanic arc in this area (Bahar and Girod, 1983; Satyana, 2007). Besides those four faults, there are several smaller faults, which include the E–W Lembang fault in West Java, the NE–SW Opak fault in Central Java and the NE–SW Grindulu fault in East Java (Fig. 2).

The volcanoes and faults on Java are host to at least 62 geothermal fields (Setijadji, 2010), most of which are located in the Quaternary volcanic arc, including 7 developed geothermal fields, i.e. Dieng, Darajat, Kamojang, Wayang-Windu, Gunung Salak, Patuha and Karaha-Bodas.

3. Sampling and analysis

Water samples were collected from July to September 2012, the end of the dry season in Java. In total 69 samples were collected, 61 from hot springs, 4 from cold springs, and 4 from hot crater lakes (Table 1). The locations of the 4 cold spring samples were chosen based on their proximity to those hot springs which were sampled during this investigation.

Temperature, pH, conductivity, ORP and alkalinity, were measured in the field, either by probe or acid titration (HACH, 2007). The samples were filtered through a 0.45 μm nylon membrane. Part of the filtered sample was used for alkalinity measurement and two splits for the determination of anion, cation and isotopic compositions were stored in polyethylene bottles and transported to the University of Bremen for further analyses. The cation split was acidified to 1% concentrated HNO_3 to avoid precipitation of metals. The anions, Cl^-, SO_4^{2-}, NO_3^- and Br^-, were analyzed by ion chromatography using an IC Plus Chromatograph (Metrohm). The cations, Ca^{2+}, Mg^{2+}, Na^+ and K^+, and Si were determined by inductively coupled plasma-optical emission spectrometry (ICP-OES) using an Optima 7300 instrument (Perkin Elmer). Trace elements of B and As were measured by using inductively coupled plasma-mass spectrometry (ICP-MS) using an iCAP-Q instrument (Thermo Fisher). Stable isotopes (^{18}O and ^2H) were determined on a LGR DLT-100 laser spectrometer (Los Gatos Research). The isotope results were reported in δ per mil (‰) relative to VSMOW with an analytical uncertainty of approximately ± 1‰ for δ^2H and ± 0.2‰ for $\delta^{18}O$.

4. Results

The results of the field and laboratory measurements are presented in Table 1. Cold water springs in Java were slightly acid to slightly alkaline (pH = 6.2 to 7.8) and conductivity ranged from 86 to 324 μS/cm. Compared to the hot spring samples, the concentrations of Ca^{2+}, Mg^{2+}, Na^+, K^+ and Cl^- of the cold spring waters were low (≤31 mg/L). These cold spring waters had HCO_3^- and SO_4^{2-} contents of 19.5 to 115.9 mg/L and 2.7 to 40.6 mg/L, respectively.

The volcano-hosted hot springs had a larger variety of temperature, pH, conductivity, major anions (HCO_3^-, SO_4^{2-}, and Cl^-) and two major cations (Na^+ and Mg^{2+}), but relatively a similar range of K^+ and a

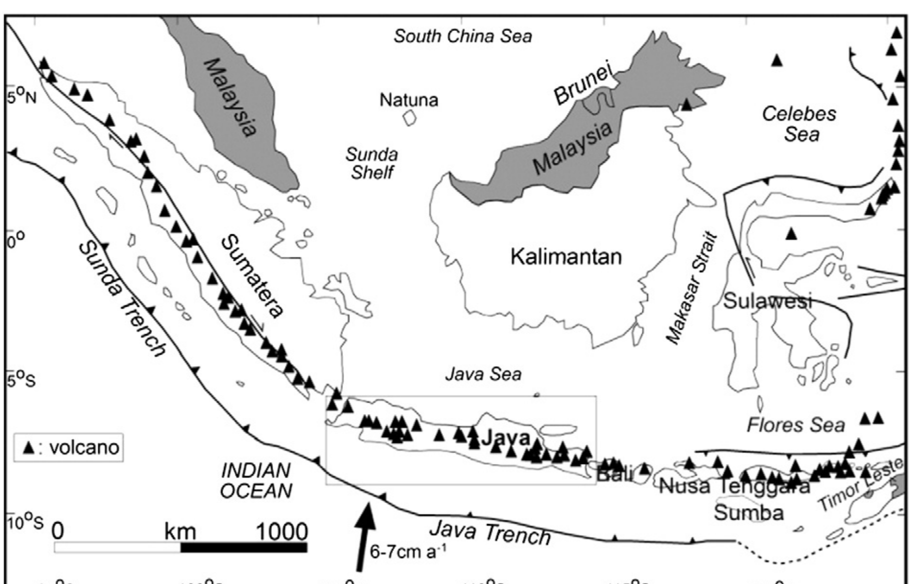

Fig. 1. Geographic and tectonic map of the Indonesian archipelago with Java in the center and the Sumatera-Nusa Tenggara volcanic arc (after Hamilton, 1979; Simandjuntak and Barber, 1996).

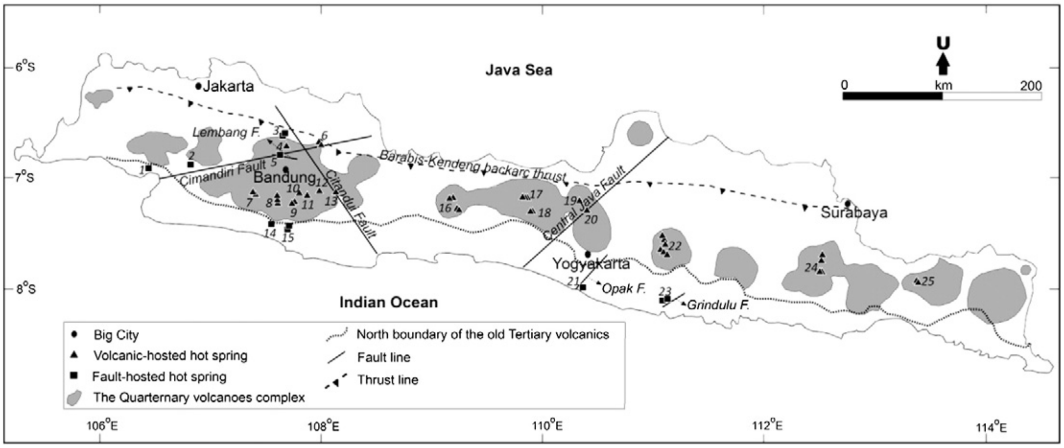

Fig. 2. The distribution of sampled geothermal systems on Java, i.e., (1) Cisolok, (2) Cikundul, (3) Batu Kapur, (4) Ciater, (5) Maribaya, (6) Tampomas, (7) Patuha, (8) Pangalengan, (9) Darajat, (10) Kamojang, (11) Cipanas, (12) Kampung Sumur, (13) Ciawi, (14) Cilayu, (15) Pakenjeng, (16) Slamet Volcano, (17) Dieng, (18) Kalianget, (19) Ungaran, (20) Candi Dukuh, (21) Parangtritis, (22) Lawu, (23) Pacitan, (24) Arjuna-Welirang and (25) Segaran. Geological structures and volcanic belts were based on Hamilton (1979), Simandjuntak and Barber (1996), Hoffmann-Rothe et al. (2001) and Soeria-Atmadja et al. (1994).

smaller range of Ca^{2+}, compared to the fault-hosted hot springs. The temperatures of the volcano-hosted hot springs ranged from 22 to 95 °C and those of the fault-hosted hot springs ranged from 47 to 102 °C. The volcano-hosted hot springs were very acid to slightly alkaline (pH = ~1 to 8.4), while the fault-hosted hot springs were slightly acid to slightly alkaline (pH = 5 to 8.1). The conductivity of the volcano-hosted hot springs varied from 86 to 14600 µS/cm, compared to 1500 to 17340 µS/cm of the fault-hosted hot springs. The concentration of HCO_3^- in the volcano-hosted hot springs ranged from below detection to 1634.8 mg/L, SO_4^{2-} ranged from below detection to 3005.5 mg/L, and Cl^- ranged from 6.9 to 8084 mg/L; and the concentration of HCO_3^- in the fault-hosted hot springs ranged from 22 to 1085.8 mg/L, SO_4^{2-} ranged from below detection to 1284.5 mg/L, and Cl^- ranged from 122.1 to 6184.5 mg/L. The concentration of Mg^{2+} in the volcano-hosted hot springs ranged from 2.6 to 211.9 mg/L, Na^+ ranged from 2.2 to 2979 mg/L, K^+ ranged from 1.4 to 119.8 mg/L, and Ca^{2+} ranged from 4.9 to 510.7 mg/L; while the concentration of Mg^{2+} in the fault-hosted hot springs ranged from below detection to 97.7 mg/L, Na^+ ranged from 115.8 to 1797.4 mg/L, K^+ ranged from below detection to 94.2 mg/L, and Ca^{2+} ranged from 32.8 to 2047.6 mg/L.

Both the volcano- and fault-hosted hot springs were characterized by relatively large variation of B, Li and As concentrations. The B concentration of the volcano-hosted systems ranged from 0.03 to 94.4 mg/L, Li ranged from 0.4 µg/L to 11.06 mg/L and As ranged from 0.3 µg/L to 9.5 mg/L. In the fault-hosted systems, the B concentrations ranged from 0.42 to 58.2 mg/L, Li ranged from 23.5 µg/L to 2.23 mg/L and As ranged from 1.2 µg/L to 3.5 mg/L. Most of the hot springs with high B, Li and As concentrations were chloride water. This phenomenon is common in geothermal systems, because neutral chloride waters ascend directly from the reservoir and thus are generally enriched in selected trace elements, i.e., the geothermal suite of elements (White et al., 1971; Nicholson, 1993; Goff and Janik, 2000).

In addition to physicochemical parameters, stable isotopes of ^2H and ^{18}O were determined. The stable isotope composition of hot spring waters from the volcano-hosted systems had a larger variation than those from the fault-hosted systems. The ^{18}O isotope composition of the cold springs ranged from −8.8 to −6.1‰, that of the volcano-hosted hot spring waters ranged from −9.3 to 7.9‰ and that of the fault-hosted hot spring waters ranged from −7.5 to −4.3‰ (Table 1). The ^2H isotope composition of the cold springs ranged from −55.6 to −42.0‰, that of the volcano-hosted hot spring waters ranged from −62.3 to −4.1‰ and that of the fault-hosted hot spring waters ranged from −50.1 to −4.2‰ (Table 1).

5. Discussion

5.1. General considerations about geothermal systems on Java

As mentioned above, geothermal systems on Java were classified into volcano-hosted and fault-hosted. Based on this classification, from a total of 25 sampled geothermal systems, 8 were considered fault-hosted (i.e., Pacitan, Maribaya, Batu Kapur, Pakenjeng, Cilayu, Cikundul, Cisolok, and Parangtritis) and 17 were considered volcano-hosted (i.e., Segaran, Arjuna-Welirang Volcano, Lawu Volcano, Ungaran Volcano, Candi Dukuh, Dieng, Kalianget, Slamet Volcano, Ciawi, Kampung Sumur, Tampomas, Cipanas, Ciater, Darajat, Kamojang, Pangalengan, and Patuha) (Fig. 2). All of the volcano-hosted geothermal systems were in the Quaternary volcanic belt, while most of the fault-hosted geothermal systems were in the Tertiary volcanic belt (Fig. 2).

Several of those fault-hosted geothermal systems are located in major fault zones, e.g. the Cisolok and Cikundul geothermal systems in the Cimandiri fault, the Maribaya geothermal system in the Lembang fault, the Parangtritis geothermal system in the Opak fault, and the Pacitan geothermal system in the Grindulu fault. The Batu Kapur, the Pakenjeng and the Cilayu geothermal systems are associated with minor faults (Fig. 2). In contrast to the other fault-hosted geothermal systems, the Maribaya and the Batu Kapur were located in the active Quarternary volcanic belt, thus probably are heated by volcanic activity. According to the geologic maps of Java (Silitonga, 1973; Alzwar et al., 1992; Samodra et al., 1992; Sujatmiko and Santosa, 1992; Effendi et al., 1998), the Pacitan, the Pakenjeng, the Cilayu, the Cisolok and the Parangtritis geothermal systems are situated close to the zones of the Tertiary intrusive rocks. The position of a fault-hosted geothermal field near an intrusive rock could be an indication of a magmatic heat source, an assumption that was further investigated using geochemical tools.

The origin and physicochemical history of hydrothermal fluids can be explored in a Cl, SO_4 and HCO_3 ternary diagram (Chang, 1984; Giggenbach, 1991; Nicholson, 1993; Giggenbach, 1997). Based on their position in the diagram, hydrothermal waters can be divided into neutral chloride, acid sulfate and bicarbonate waters, but mixtures of the individual groups are common. On Java, bicarbonate was the dominant water type for the volcano-hosted hot springs, followed by acid sulfate and neutral chloride waters, while for the fault-hosted hot springs the water types were distributed more or less evenly (Fig. 3). The occurrence of different water types in a given hydrothermal system is common, indicating the different physicochemical processes, such as, phase separation and mixing in the shallow subsurface (Ellis and Mahon, 1977; Henley and Ellis, 1983; Hedenquist, 1990; Giggenbach, 1997; McCarthy et al., 2005). Although the bicarbonate water type

Table 1
Sampling locations, physicochemical and stable isotope compositions of cold springs, hot springs and hot acid crater lakes on the island of Java.

Sample ID	Location	Geo. Type	Temp. (°C)	pH	Ec (uS/cm)	TDS (mg/L)	Ca	Mg	Na	K	Cl	HCO_3	SO_4	NO_3	Br	Si	B	Li (µg/L)	As	^{18}O (‰)	^{2}H
Hot springs																					
J1	Pancuran 3 (Slamet volc.)	V	46.3	6.2	4070	3995	189.6	204.2	358.0	75.4	732.5	652.7	599.6	<dl	<dl	85.1	4.01	19.6	12.1	−8.6	−61.9
J2	Pancuran 7 (Slamet volc.)	V	52.1	6.9	4280	3200	201.2	209.2	371.5	75.3	777.3	722.2	614.7	<dl	<dl	89.6	4.33	76.8	12.7	−9.1	−60.6
J3	Ciawi 1	V	43.2	6.5	1500	1123	73.0	61.3	169.1	43.0	152.7	844.2	<dl	<dl	<dl	86.7	5.90	478.5	17.8	−6.4	−36.4
J4	Ciawi 2	V	53.4	6.7	1860	1300	85.8	72.5	197.9	48.4	165.3	976.0	<dl	<dl	<dl	91.3	6.84	534.4	18.3	−6.2	−38.9
J6	Ciengang (Cipanas)	V	46.2	6.2	1525	1048	72.6	90.7	121.9	25.0	113.6	362.3	453.4	<dl	<dl	67.2	2.16	96.7	5.5	−7.4	−48.4
J7	Cipanas Indah (Cipanas)	V	48.3	6.3	1632	1132	68.7	107.0	143.8	28.6	119.0	383.1	486.4	<dl	<dl	68.6	2.43	123.4	6.6	−7.5	−49.8
J8	Tirtagangga (Cipanas)	V	49.3	6.4	1655	1170	80.4	100.3	138.2	27.2	119.0	397.7	513.8	<dl	<dl	70.2	2.51	96.3	4.7	−7.8	−49.7
J10	Kawah Hujan (Kamojang)	V	95.4	4.9	618	409	25.1	5.9	19.5	6.9	7.2	22.0	133.4	0.8	<dl	83.9	4.63	0.4	3.1	−1.3	−21.4
J11	Tirtahusada (Pacitan)	F	51.3	5.0	4262	3055	417.2	<dl	200.2	<dl	308.2	23.2	1127.9	<dl	<dl	16.4	0.42	23.5	30.5	−5.7	−39.5
J12	Tinatar (Pacitan)	F	37.3	6.9	2862	2115	484.3	2.0	185.3	<dl	308.2	22.0	1284.5	<dl	<dl	16.6	0.42	26.6	23.2	−6.2	−35.8
J13	Padusan 1 (Arjuna-Welirang volc.)	V	48.3	6.5	2574	1882	142.4	108.5	239.9	56.8	246.2	1104.1	171.7	<dl	<dl	74.9	4.97	166.9	15.1	−9.3	−62.4
J14	Padusan 2 (Arjuna-Welirang volc.)	V	45.7	6.3	2377	1730	119.5	86.8	192.9	46.2	206.3	1000.4	140.4	3.9	<dl	65.0	4.14	130.8	14.0	−9.3	−59.3
J16	Cangar 1 (Arjuna-Welirang volc.)	V	46.1	6.8	1336	918	72.0	87.3	116.4	31.0	48.1	695.4	82.6	14.2	<dl	49.9	2.62	1.6	2.6	−8.5	−60.9
J17	Cangar 2 (Arjuna-Welirang volc.)	V	42.3	6.7	887	599	56.0	43.9	78.2	21.0	38.2	597.8	61.9	15.8	<dl	48.8	2.00	1.3	1.8	−9.1	−58.4
J18	Songgoriti 1 (Arjuna-Welirang volc.)	V	46.4	6.3	5470	4178	170.3	124.8	765.2	52.9	1303.5	1378.6	<dl	<dl	<dl	84.9	50.56	1710.4	4448.8	−5.9	−46.2
J19	Songgoriti 2 (Arjuna-Welirang volc.)	V	28.4	7.0	5549	4342	172.2	130.9	797.5	55.6	1366.8	1134.6	<dl	<dl	<dl	86.2	51.84	1784.4	1423.1	−4.8	−44.1
J20	Songgoriti 3 (Arjuna-Welirang volc.)	V	41.5	6.3	4658	3514	145.0	105.3	635.6	44.7	1084.4	1146.8	<dl	<dl	<dl	80.0	42.04	1437.2	777.6	−6.1	−45.3
J21	Segaran 1 (Lamongan volc.)	V	44.9	6.5	3907	2892	100.7	211.9	405.3	79.3	550.5	1625.0	<dl	<dl	<dl	73.9	21.37	619.2	46.6	−5.0	−29.9
J22	Segaran 2 (Lamongan volc.)	V	22.3	6.3	3504	2582	91.9	186.8	362.7	71.8	497.9	1457.9	<dl	3.9	<dl	70.5	18.74	549.0	50.8	−5.0	−30.2
J23	Cumpleng (Lawu volc.)	V	34.3	6.2	2301	1678	73.3	33.0	394.5	12.2	300.0	971.1	7.4	<dl	<dl	52.5	4.08	682.8	21.9	−6.4	−42.9
J24	Banyuasin (Lawu volc.)	V	38.4	6.1	13800	12040	510.7	146.2	2979.0	119.8	5948.7	835.7	256.4	<dl	13.0	42.9	93.23	11060.5	9514.8	−4.0	−42.4
J26	Pablengan (Lawu volc.)	V	36.4	6.3	14600	12750	139.5	46.4	2967.1	81.4	4382.4	1634.8	<dl	<dl	11.3	49.6	55.60	3448.9	229.5	−3.4	−31.7
J27	Ngerak (Lawu volc.)	V	34.4	6.2	2756	2032	196.0	84.1	191.8	39.9	668.9	151.3	248.3	5.1	<dl	52.5	5.22	108.1	6.8	−8.9	−59.4
J28	Kondo (Lawu volc.)	V	33.2	6.4	4860	3745	159.4	46.7	841.8	22.4	904.9	878.4	511.9	<dl	<dl	30.1	17.37	1127.6	49.5	−5.4	−39.6
J29	Bayanan (Lawu volc.)	V	39.8	6.8	2330	1688	103.6	69.9	289.8	29.1	323.8	988.2	<dl	<dl	<dl	69.4	3.34	297.6	0.9	−6.1	−36.5
J30	Ngunut (Lawu volc.)	V	41.0	6.6	2451	1784	98.2	77.7	316.6	25.4	333.1	1030.9	<dl	<dl	<dl	73.1	3.47	359.6	0.9	−6.3	−37.0
J31	Candi Dukuh (Ambarawa)	V	35.9	7.2	1168	806	46.0	38.0	162.9	14.0	171.3	377.0	<dl	<dl	<dl	37.6	3.80	74.6	35.8	−6.5	−44.6
J32	Candi Songo (Ungaran volc.)	V	48.5	3.0	870	582	24.2	10.0	18.9	9.3	14.0	<dl	340.6	1.0	<dl	83.4	0.03	6.1	3.8	−4.8	−36.3
J33	Gucci (Slamet volc.)	V	40.5	6.3	694	464	35.0	41.6	57.5	24.0	33.5	319.6	54.2	8.9	<dl	59.9	2.66	19.6	5.3	−8.7	−60.4
J34	Pengasihan (Slamet volc.)	V	53.3	7.5	1206	819	46.0	56.5	144.5	41.0	52.6	556.3	92.0	<dl	<dl	75.4	7.15	76.8	7.9	−8.3	−63.8
J35	Maribaya	F	46.5	6.2	2345	1660	129.0	97.7	115.8	26.4	122.1	1017.5	<dl	<dl	<dl	82.5	1.94	116.5	1.2	−7.5	−50.1
J36	Ciater	V	46.6	2.0	6311	4850	88.6	30.0	58.7	41.4	822.5	<dl	659.2	6.0	<dl	78.7	2.07	37.6	68.3	−6.9	−44.6
J37	Batu Kapur 1	F	56.3	6.7	2154	1530	50.6	46.2	310.4	58.5	280.4	717.4	75.4	<dl	<dl	87.9	2.74	539.7	1.3	−7.1	−41.4
J38	Batu Kapur 2	F	40.9	6.4	2486	1802	102.1	96.6	276.9	39.9	312.7	1085.8	<dl	<dl	<dl	75.1	3.12	703.4	2.5	−6.4	−39.3
J39	Cibolang (Pangalengan)	V	68.9	7.1	988	650	77.0	43.0	71.3	28.0	24.0	219.6	236.0	<dl	<dl	95.5	6.48	63.8	14.2	−6.5	−47.3

J40	Sukaratu (Pangalengan)	V	39.8	6.4	1005	682	64.0	53.2	97.8	14.0	18.6	475.8	102.6	<dl	<dl	70.1	2.12	61.5	6.2	−8.1	−56.1
J41	Kertamanah (Pangalengan)	V	54.1	6.4	3208	553	54.0	35.7	94.4	26.0	17.6	433.1	91.8	<dl	<dl	92.5	1.06	56.1	35.8	−8.1	−53.3
J42	Pakenjeng	F	59.9	7.4	1960	1367	225.5	<dl	224.3	<dl	126.0	40.3	940.2	<dl	<dl	27.1	7.21	92.8	685.4	−6.5	−35.6
J43	Pakenjeng	F	43.1	7.5	2048	1461	215.6	<dl	256.9	<dl	131.7	42.7	960.0	<dl	<dl	26.6	7.68	72.4	699.7	−6.2	−35.8
J44	Cilayu	F	70.3	8.1	5892	4435	68.3	12.9	1101.5	66.1	1387.2	372.1	408.1	<dl	4.9	79.4	58.22	2233.0	3521.5	−5.3	−40.8
J45	Cilayu	F	45.1	7.9	10140	8316	227.0	9.9	1797.4	94.2	3210.5	289.1	156.6	<dl	11.1	82.8	47.57	1780.6	2779.3	−5.3	−33.9
J46	Kalianget	V	38.9	6.6	2611	1927	118.2	150.7	190.1	45.3	399.1	844.2	150.8	<dl	<dl	61.7	3.52	203.4	135.9	−9.1	−58.4
J47	Kalianget	V	40.0	6.5	2657	1954	128.3	156.7	197.5	49.3	424.8	732.0	163.6	<dl	<dl	66.2	3.73	208.3	189.3	−9.0	−59.5
J48	Cikundul	F	50.5	7.8	1500	1026	32.8	1.1	264.3	5.4	180.2	61.0	374.2	<dl	<dl	37.6	10.72	94.2	38.8	−5.7	−39.4
J49	Cisolok	F	102.0	8.1	1705	1180	41.2	3.0	285.8	10.3	305.6	129.3	235.5	<dl	<dl	66.3	3.58	290.1	104.0	−5.9	−33.0
J50	Cisolok	F	100.0	8.0	1612	1078	52.3	3.3	257.6	8.8	277.0	161.0	222.7	<dl	<dl	58.9	3.20	251.9	96.1	−6.0	−35.3
J52	Patuha	V	64.3	8.4	715	468	41.6	16.7	71.4	16.5	35.2	300.1	46.9	<dl	<dl	80.7	1.29	44.9	43.1	−8.9	−56.6
J53	Tampomas	V	51.4	6.9	1912	1349	73.2	50.8	241.9	22.8	280.2	705.2	1.6	<dl	<dl	90.8	4.95	490.5	0.7	−6.2	−42.8
J54	Tampomas	V	48.5	7.1	3462	2526	83.4	50.6	542.2	30.2	757.2	732.0	<dl	<dl	2.8	82.7	5.28	1523.0	2.1	−6.6	−41.2
J55	Darajat	V	60.0	2.8	952	643	13.7	5.3	7.9	2.9	13.3	<dl	254.1	1.0	<dl	78.8	6.97	2.9	87.2	−7.9	−50.6
J56	Darajat	V	54.0	3.8	344	222	24.0	4.3	10.9	5.0	6.9	<dl	117.6	0.6	<dl	49.7	1.11	5.8	17.1	−8.7	−51.9
J57	Kampung Sumur	V	35.0	7.6	592	399	19.0	18.1	85.9	14.0	52.0	229.4	13.9	0.9	<dl	43.0	0.95	33.1	10.2	−7.5	−47.2
J58	Parangtritis	F	39.2	7.6	17340	15430	2047.6	8.7	1640.0	21.4	6184.5	43.9	477.0	<dl	18.1	26.2	9.51	282.3	15.6	−4.3	−24.2
J60	Dieng	V	57.4	6.3	1104	762	60.0	19.5	112.4	27.0	77.7	266.0	202.9	0.8	<dl	49.5	6.67	13.8	6.1	−4.3	−47.4
J61	Dieng	V	54.0	6.2	1550	1082	130.4	40.2	104.1	59.1	330.6	183.0	67.8	<dl	1.0	103.5	6.41	52.8	2.1	−8.0	−57.2
J62	Dieng	V	70.1	6.8	343	216	23.8	11.2	16.6	20.3	9.0	124.4	16.6	<dl	<dl	97.9	0.09	2.5	91.1	−8.6	−57.6
J63	Dieng	V	56.1	6.7	745	487	41.9	25.1	76.0	26.5	27.3	270.8	119.7	<dl	<dl	91.6	4.55	22.6	2.3	−7.3	−55.6
J64	Dieng	V	60.0	7.3	744	487	41.7	14.3	95.5	32.2	21.5	329.4	82.8	0.9	<dl	81.4	2.08	45.0	6.6	−8.0	−57.1
J65	Dieng	V	81.0	7.3	1575	1046	16.3	6.6	4.0	2.2	14.7	104.9	298.5	1.3	<dl	13.2	0.54	6.7	1.2	0.6	−21.0
J66	Dieng	V	31.6	5.9	427	283	35.6	21.6	15.7	11.2	15.7	201.3	22.4	0.5	<dl	55.8	0.27	11.2	3.8	−8.2	−54.8
J68	Dieng	V	23.4	2.5	1748	1260	4.9	2.6	2.2	1.4	13.1	<dl	434.0	0.9	<dl	45.4	0.15	3.6	2.4	−8.6	−54.3
J69	Dieng	V	26.6	6.0	400	267	35.2	24.3	10.9	8.1	16.8	179.3	41.2	<dl	<dl	52.0	0.17	4.4	0.3	−9.3	−62.3
Hot crater lakes																					
J9	Kamojang	V	40.0	2.9	1185	826	63.0	23.5	15.9	23.0	12.8	<dl	406.8	<dl	<dl	168.8	1.39	13.3	1.3	7.7	−4.1
J51	Patuha	V	32.9	1.0	86	115	75.0	32.1	34.2	33.0	8084.2	<dl	3005.5	0.7	20.5	122.4	94.40	41.7	236.5	7.9	−4.0
J59	Dieng	V	86.8	2.5	2569	1851	18.3	14.5	11.4	5.9	14.4	<dl	900.6	<dl	<dl	161.5	73.29	12.6	1.4	7.5	-7.6
Cold springs																					
J5	Ciawi	–	25.2	6.5	169	108.1	15.0	9.5	2.9	<dl	9.1	97.6	2.7	0.9	<dl	36.0	0.01	2.7	0.9	−6.1	−42.0
J15	Arjuna-Welirang	–	22.6	6.3	324	215.0	31.0	13.6	16.0	5.0	22.0	115.9	30.4	8.2	<dl	30.7	0.27	2.6	2.9	−7.6	−52.5
J25	Lawu	–	21.9	6.2	86	55.3	5.0	1.6	9.5	<dl	9.5	19.5	12.7	2.2	<dl	20.5	0.10	22.0	73.2	−7.9	−52.8
J67	Dieng	–	18.1	7.6	286	190.4	28.8	6.6	13.5	4.8	15.6	15.9	40.6	48.4	<dl	21.6	0.97	1.4	0.9	−8.8	−55.6
Seawater																					
SW	Indian Ocean	–	nm	nm	nm	nm	369.7	1372.8	10683	360	19191	151	2183	<dl	60.3	nm	9.96	11.6	nm	nm	nm

V = volcano-hosted, F = fault-hosted, volc. = volcano, <dl = below detection limit, nm = not measured.

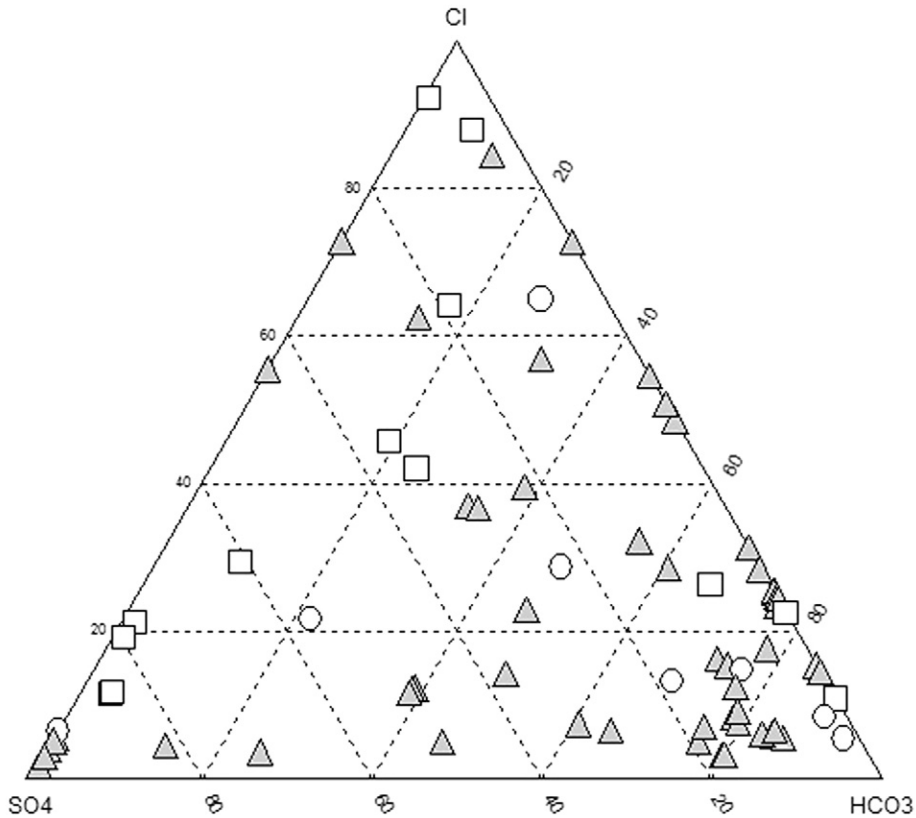

Fig. 3. SO_4-HCO_3-Cl ternary diagram of cold and hot springs. Most of the volcano-hosted hot springs were of the HCO_3^- water type, whereas the fault-hosted hot springs were distributed evenly between the $SO4^{2-}$, HCO_3^- and Cl^- types. Open circle = cold spring, gray filled triangle = volcano-hosted hot spring and open square = fault-hosted hot spring.

seems to be more abundant in the volcano-hosted hydrothermal systems, a definite difference between the volcano- and fault-hosted systems is difficult to be assessed in a ternary diagram alone. Thus, following the procedure of Valentino and Stanzione (2003), the hot waters from Java were plotted in HCO_3 vs. Cl and Mg/Na vs. SO_4/Cl diagrams (Figs. 4 and 5). These diagrams show that the volcano-hosted thermal waters have a higher HCO_3^- content and a higher Mg^{2+}/Na^+ ratio. This observation could be the result of magmatic degassing and thus addition of CO_2 to the volcano-hosted hot springs, which is likely absent or minor in the fault-hosted hot springs. The reaction between H_2O and CO_2 increases acidity and thus intensifies water–rock interaction (White, 1957; Giggenbach, 1984; Giggenbach, 1988). Acid conditions and low temperature, due to slow upward migration or a long flow path of the ascending thermal waters, increases the solubility of Mg^{2+} (Allen and Day, 1927), hence producing Mg-rich waters.

Four groups of the volcano-hosted thermal waters are shown in the HCO_3 vs. Cl and the Mg/Na vs. SO_4/Cl diagrams, i.e., A, B, C and D (Figs. 4 and 5). The group A samples had the highest HCO_3^- and Cl^- concentrations, but the lowest SO_4/Cl ratios. Conversely, the group D samples had the lowest HCO_3^- and Cl^- concentrations but the highest SO_4/Cl ratios. Meanwhile, groups B and C had HCO_3^- and Cl^- concentrations and SO_4/Cl ratios in between those of groups A and D. However, group C was split from group B due to its lower HCO_3^- and Cl^- contents. Groups A and B are thought to have formed at the margin of the 'primary neutralization' zone (Giggenbach, 1988). There separation of CO_2 and its reaction with groundwater produces HCO_3-rich thermal waters, while the Cl^- content remains high due to the lesser dilution by groundwater. The group A samples originated closer to the 'primary neutralization' zone than the group B samples and thus had a higher Cl^- concentration. In the Mg/Na vs. SO_4/Cl diagram, two acid thermal waters, J51 (Kawah Putih) and J36 (Ciater), are exceptions in group B. The moderate SO_4^{2-}/Cl^- ratios in these two samples were likely caused by H_2S and HCl addition to shallow groundwater (Giggenbach, 1988; Delmelle and Bernard, 1994; Delmelle et al., 2000; Sriwana et al., 2000). The resulting low pH enhances water–rock interaction, thus causing the high Mg^{2+}/Na^+ ratio in those two samples. The group C samples were considered thermal waters formed in the shallow subsurface and thus were diluted by groundwater, which lowered their HCO_3^- and Cl^- contents. The group D samples were interpreted to be thermal waters influenced by primary H_2S-rich magmatic vapor in the shallow subsurface, hence producing acid sulfate waters. In this group, J65 (Dieng) was an exception (Fig. 5), because the hot spring had a neutral (pH = 7) and was Cl-poor (14.7 mg/L). This thermal water is likely a mixture of HCO_3-rich and SO_4-rich water, which can occur in low relief liquid-dominated geothermal systems (Kuhn, 2004). Meanwhile, the thermal waters of the fault-hosted geothermal systems were divided into two groups, E and F, where the former had a higher Cl^- content than the latter. Chloride is a conservative element and thus the Cl^- variation in the fault-hosted thermal waters could have been caused by either varying degrees of mixing with shallow groundwater or a reflection of the initial Cl^- content of the hydrothermal fluid. Based on that assumption, group E thermal waters should have undergone less mixing with shallow groundwater than group F. This is also indicated in the Na–K–Mg ternary diagram (Giggenbach, 1988), where the group E thermal waters (J45 and J58) plot closer to equilibrium than the group F thermal waters (Fig. 7). The high Cl^- concentration in sample J58 from the Parangtritis hot spring is unusual, but can be explained by seawater addition to the geothermal system, because of its proximity to the Indian Ocean. Most of the acid sulfate waters had HCO_3^- concentrations, which were below detection and thus fewer samples could be plotted as group D in the HCO_3 vs. Cl diagram than in the Mg/Na vs. SO_4/Cl diagram. Conversely, many neutral chloride waters were below the detection limit of SO_4^{2-} and therefore more thermal waters plotted as group A in the HCO_3 vs. Cl diagram than in the Mg/Na vs. SO_4/Cl diagram.

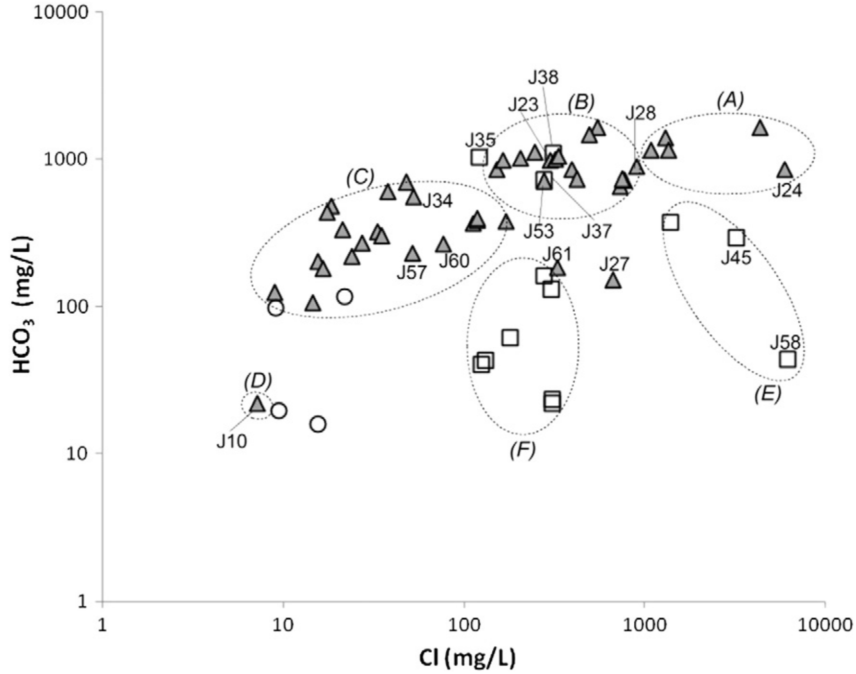

Fig. 4. HCO_3 vs. Cl (in mg/L basis) diagram of cold and hot springs for: (A) and (B) formed in the margin of the 'primary neutralization', where (A) is closer than (B), (C) thermal waters from shallow depth, thus underwent major dilution by groundwater, (D) volcanic H_2S gas oxidized by O_2-rich groundwater, (E) and (F) fault-hosted hot springs, where (E) is less diluted by groundwater than the (F). (E) is likely influenced by seawater input. (Symbols are as in Fig. 3).

Several anomalies and discrepancies were found in both the HCO_3 vs. Cl and Mg/Na vs. SO_4/Cl diagrams. In the HCO_3 vs. Cl diagram, the fault-hosted hot springs of Maribaya (J35) and Batu Kapur (J37 and J38) plot within the group B of the volcano-hosted thermal waters, whereas the volcano-hosted hot springs of J27 (Lawu) and J61 (Dieng) plot as a group of fault-hosted thermal waters (Fig. 4). As mentioned previously, the HCO_3^- abundance in the Maribaya and Batu Kapur hot springs was likely caused by addition of magmatic CO_2, due to their location within the active Quaternary volcanic belt. Meanwhile, the lower HCO_3^- concentrations in samples J27 (Lawu) and J61 (Dieng) were likely the result of carbonate mineral precipitation. That sample J28 plots below group B in the Mg/Na vs. SO_4/Cl diagram should be due to the formation of clay minerals and the associated depletion of Mg^{2+}. The discrepancy that samples J23 and J53 plot in group B in the HCO_3 vs. Cl diagram and in group A in the Mg/Na vs. SO_4/Cl diagram can be attributed to the removal of SO_4 due to precipitation of sulfate

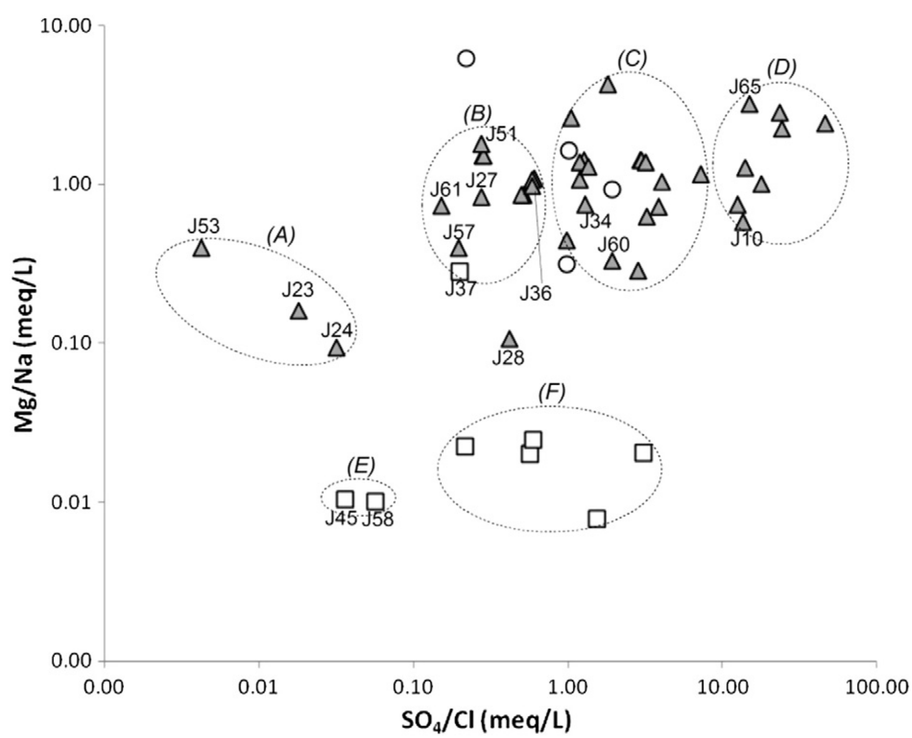

Fig. 5. Mg/Na vs. SO_4/Cl (in meq/L basis) diagram of cold and hot springs. The interpretation of groups A, B, C, D, E and F are similar to that in Fig. 4. (Symbols are as in Fig. 3.)

minerals. The same process is the likely cause for the location of sample J57, a dilute thermal water, in group B in the Mg/Na vs. SO_4/Cl diagram.

The Cl/B ratios of hydrothermal waters can be used to identify subsurface processes, such as, water–rock interaction, magma degassing and seawater feeding in a geothermal system (Arnorsson and Andresdottir, 1995; Valentino and Stanzione, 2003). The Cl/B ratios found in the samples from Java indicated three dominant processes for the volcano-hosted thermal waters, i.e., groundwater mixing, water–rock interaction with the andesitic host rock and phase separation. On the other hand, the Cl/B ratios of fault-hosted hot springs were generally affected by water–rock interaction with the andesitic host rock (Fig. 6).

Geothermal water in the Dieng, Kamojang and Darajat geothermal fields had lower Cl/B ratio than the andesitic rock (Fig. 6), something that can be caused by phase separation in high temperature (>300 °C) reservoirs (Truesdell et al., 1989). This process removes B from the geothermal reservoir, thus relatively increasing the Cl^- concentration of the remaining hydrothermal fluid (Truesdell et al., 1989; Arnorsson and Andresdottir, 1995). One volcano-hosted hot spring, J36 (Ciater), and three fault-hosted hot springs, J11 (Pacitan), J12 (Pacitan) and J58 (Parangtritis), plotted closed to the seawater-precipitation line. The J58 (Parangtritis) sample also plotted in the HCO_3 vs. Cl and Mg/Na vs. SO_4/Cl diagrams in a way which would indicate seawater addition. However, seawater addition is not likely for the J12 and J13 hot springs due to their low Cl^- concentration. Hence, the low B/Cl ratio of these hot springs could have been caused by B removal due to adsorption by clay minerals, particularly illite (Harder, 1970).

5.2. Geothermometry

Solute geothermometers, such as those listed in Table 2, can provide powerful tools to estimate subsurface conditions. Their successful application has been extensively discussed in the geothermal literature and relies on five basic assumptions: 1) exclusively temperature dependent mineral–fluid reaction; 2) abundance of the mineral and/or solute; 3) chemical equilibrium; 4) no re-equilibration; and 5) no mixing or dilution (e.g., Nicholson, 1993). The no mixing or dilution assumption, however, can be circumvented if its extent and/or influence on solute ratios (e.g., Na/K) are known. Several geothermometers were applied in order to analyze the physichochemical processes encountered by the hydrothermal fluids during their ascent to the surface. These processes include dilution by shallow water, conductive cooling, adiabatic cooling, mineral precipitation, adsorption/desorption, water–rock interaction and re-equlibrium (Fournier, 1977; Kaasalainen and Stefánsson, 2012). Different geothermometers record different equilibria and disagreement does not immediately eliminate the use of one or the other. Careful application and evaluation of calculated temperatures may provide important clues to the overall hydrology of the geothermal system (Pichler et al., 1999).

Silica geothermometers, which are commonly applied to hot springs (Fournier, 1977) predicted a temperature range from 100 to 140 °C for most samples (Table 2). Lower temperatures were calculated for J60 (Kampung Sumur), J31 (Candi Dukuh), and J24 and J28 (Lawu). The J60 and J31 hot springs were located at the edge of a pool and a lake, respectively and thus, should be diluted by surface water. The two hot springs, J24 and J28, were Cl-rich, which would preclude dilution by surface or groundwater dilution. That led to the conclusion that the J24 and J28 hot springs lost silica due to the precipitation of silicate minerals during ascent, causing the low silica geothermometer temperatures.

When applied to hot springs, silica thermometers are known to predict closer to the discharge temperature, rather than the reservoir temperature (e.g., Pichler et al., 1999). This inherent problem can be overcome by calculating the silica 'parent' concentration using the silica mixing model of Fournier (1977). After application, the silica geothermometers predicted much higher reservoir temperatures of 258 °C for Slamet, 188 °C for Ciawi, 180 °C for Batu Kapur and 221 °C for Pangalengan. These temperatures were in the range of those predicted by the Na/K and Na/K/Ca geothermometers (see below).

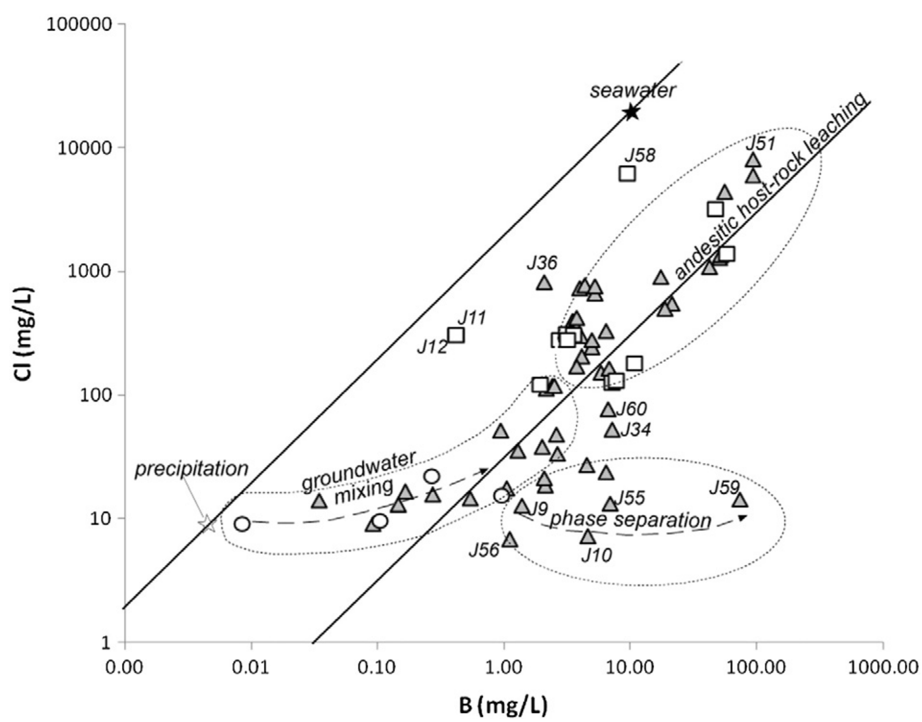

Fig. 6. Cl vs. B diagram of cold waters and geothermal waters. The Cl/B ratio of seawater from the Indian Ocean (this research) and andesitic rock from Trompetter et al. (1999) are used. The Cl/B ratio of volcano-hosted and fault-hosted hot springs were considered to be controlled by water–rock interaction. The Dieng, Kamojang and Darajat volcano-hosted geothermal systems underwent phase separation. Though J58 (Parangtritis), J11 and J12 of Pacitan and J36 (Ciater) plotted close to seawater, seawater mixing was indicated only for J58. (Symbols are as in Fig. 3.)

Table 2
Calculated reservoir temperatures.

Location	Samples	Geothermal types	T field (°C)	Geothermometers (°C)					
	ID			Quartz	Quartz (steam loss)	Chalcedony	Quartz (parents)	Na/K	Na–K–Ca
Slamet	J1	V	46.3	128	125	101	258	290	217
	J2		52.1	131	128	104		286	215
	J33		40.5	110	110	81		380	241
	J34		53.3	122	120	94		326	232
Ciawi	J3	V	43.2	129	126	102	188	313	223
	J4		53.4	132	128	105		308	222
Cipanas	J6	V	46.2	116	115	87	nd	287	203
	J7		48.3	117	116	88		284	205
	J8		49.3	118	117	90		283	202
Arjuna-Welirang	J13	V	48.3	122	119	93	nd	304	219
	J14		45.7	114	113	85		305	217
	J16		46.1	102	102	72		318	218
	J17		42.3	101	102	71		319	213
	J18		46.4	128	125	101		187	169
	J19		28.4	129	126	101		188	180
	J20		41.5	125	122	97		189	168
Segaran	J21	V	44.9	121	119	93	nd	282	222
	J22		22.3	118	117	90		283	221
Lawu	J23	V	34.3	104	104	74	nd	133	128
	J24		38.4	95	96	64		150	155
	J26		36.4	101	102	71		127	147
	J27		34.4	104	104	74		289	203
	J28		33.2	79	83	48		125	126
	J29		39.8	118	116	89		217	176
	J30		41.0	120	118	92		199	166
Candi Dukuh	J31	V	35.9	89	91	58	nd	204	165
Pangalengan	J39	V	68.9	135	131	108	221	371	232
	J40		39.8	118	117	90		250	180
	J41		54.1	133	129	106		323	219
Kalianget	J46	V	38.9	112	111	83	nd	305	216
	J47		40.0	115	114	86		310	219
Patuha	J52	V	32.9	125	123	98	nd	301	205
Tampomas	J53	V	64.3	132	128	105	nd	212	172
	J54		51.4	127	124	99		171	158
Kampung Sumur	J57	V	35.0	95	96	64	nd	263	196
Dieng	J60	V	57	101	102	71	nd	306	213
	J61		54	139	134	113		431	261
	J62		70	136	132	109		599	296
	J63		56	132	129	105		354	233
	J64		60	126	123	98		349	236
	J66		32	107	107	77		474	248
	J69		27	104	104	74		481	242
Pacitan	J11	F	51.3	56	62	24	nd	nd	nd
	J12		37.3	54	63	24			
Maribaya	J35	F	46.5	127	124	99	nd	299	203
Batu Kapur	J37	F	56.3	130	127	103	180	278	221
	J38		40.9	122	120	93		250	195
Pakenjeng	J42	F	59.9	75	79	44	nd	nd	nd
	J43		43.1	74	79	43			
Cilayu	J44	F	70.3	125	122	97	nd	177	176
	J45		45.1	127	124	99		167	167
Cikundul	J48	F	50.5	89	91	58	nd	111	111
Cisolok	J49	F	102.0	115	114	87	nd	143	133
	J50		100.0	110	109	80		139	128
Parangtritis	J58	F	39.2	74	78	42	nd	88	55

V = volcano-hosted, F = fault-hosted, nd = not defined.

Reservoir temperature calculations with the Na/K and Na/K/Ca geothermometers were conducted according to Giggenbach (1988), by first evaluating if equilibrium between host-rock and hydrothermal fluid was attained. Only six samples, J24 and J26 (Lawu volcano), J44 and J45 (Cilayu), J48 (Cikundul), and J58 (Parangtritis) were in partial equilibrium, and four samples, J23 and J28 (Lawu), and J49 and J50 (Cisolok) were close to partial equilibrium with their respective host rocks (Fig. 7). The Na/K geothermometer was then applied for these ten samples and calculated reservoir temperatures were 127 to 150 °C for Lawu, 167 to 177 °C for Cilayu, 111 °C for Cikundul, 88 °C for Parangtritis and 139 to 143 °C for Cisolok.

Fournier (1989) proposed the use of the Na/K geothermometer and the Na–K–Ca geothermometer respectively for the prediction of the highest and the lowest reservoir temperatures in a geothermal system. Following this approach, calculated temperatures ranged from 205 to 301 °C in Patuha and 219 to 323 °C in Pangalengan geothermal systems. These results were in good agreement with the predicted reservoir temperatures by direct measurement, i.e., 209 to 241 °C for Patuha (Layman and Soemarinda, 2003) and 250 to 300 °C for Pangalengan (Layman and Soemarinda, 2003; Abrenica et al., 2010). Reliable reservoir temperature prediction with those two geothermometers was also indicated in the Dieng geothermal system, where calculated temperatures ranged

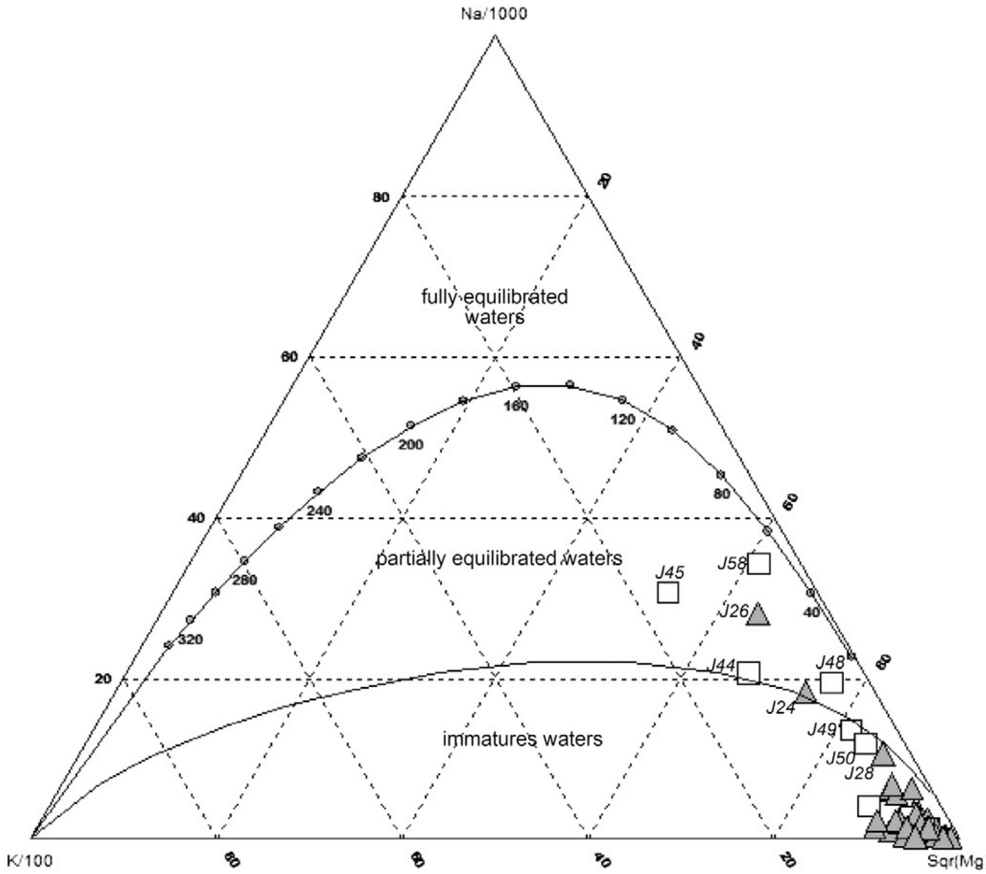

Fig. 7. Na–K–Mg ternary diagram Giggenbach (1988) for the Java hot springs. Several fault-hosted and a few volcano-hosted hot springs were close to or in partial equilibrium with the host-rock. (Symbols are as in Fig. 3.)

from 236 to 349 °C. These temperatures were relatively similar to the predictions by Prasetio et al. (2010) (i.e., 240 to 333 °C), who used gas geothermometers. Therefore, based on those observations, the two geothermometers were applied to the remaining geothermal systems and calculated temperatures in Arjuna-Welirang ranged from 217 to 305 °C, in Cipanas from 202 to 277 °C, in Segaran from 221 to 283 °C, in Kalianget from 216 to 305 °C, in Tampomas from 172 to 212 °C and in Maribaya from 203 to 299 °C.

The K^+ concentration in the Pacitan and Pakenjeng hot spring waters were below detection limit, thus the Na/K and Na/K/Ca geothermometers could not be applied. Silica geothermometers resulted in a maximum temperature of 63 °C for Pacitan and 79 °C for Pakenjeng geothermal systems. Those temperatures although likely lower than the actual reservoir temperatures indicated reservoir temperatures below 100 °C. A compilation of all calculated reservoir temperatures on Java are presented in Table 3.

In the Darajat and Kamojang geothermal systems, the only surface expressions were acid sulfate-type hot springs. That type of hydrothermal fluid reacts extensively with near surface rocks, hence chemical geothermometers could not be applied (e.g. Nicholson, 1993). A reservoir temperature of 280 °C was predicted by Hadi (1997) for the Darajat geothermal system, based on the alteration minerals observed in drill cores and Sudarman et al. (1995) reported a shallow reservoir temperature measurement of 232 °C for the Kamojang geothermal system.

5.3. The heat sources of the fault-hosted geothermal systems

The Quaternary volcanic arc could be the heat source for the fault-hosted geothermal systems. That case was investigated by comparing the enrichment of conservative trace elements and reservoir temperatures between the volcanic and fault-hosted geothermal fields. A similar procedure was applied to the Steamboat geothermal system (Arehart et al., 2003), which pointed towards a magmatic heat source rather than just enhanced heat flow. Lithium was considered as the most conservative trace element in this study, because the B concentration in several hot spring waters were affected by phase separation.

The Li vs. Cl diagram shows that some of the fault-hosted hot springs have similar high trends of Li enrichment as the volcano-hosted hot

Table 3
Compilation of calculated geothermal reservoir temperatures on Java.

Geothermal systems	Geothermal types	T (°C)	Geothermometer
Slamet M.	V	258 to 380	Si parent and Na–K
Ciawi	V	188 to 313	Si parent and Na–K
Cipanas	V	202 to 287	Na–K and Na–K–Ca
Arjuna-Welirang M.	V	217 to 305	Na–K and Na–K–Ca
Segaran	V	221 to 283	Na–K and Na–K–Ca
Lawu M.	V	127 to 150	Na–K
Candi Dukuh	V	165 to 204	Na–K and Na–K–Ca
Pangalengan	V	221 to 323	Si parent and Na–K
Kalianget	V	216 to 310	Na–K and Na–K–Ca
Patuha	V	205 to 301	Na–K and Na–K–Ca
Tampomas	V	172 to 212	Na–K and Na–K–Ca
Kampung Sumur	V	196 to 263	Na–K and Na–K–Ca
Dieng	V	236 to 349	Na–K and Na–K–Ca
Pacitan	V	<100	Si
Maribaya	F	203 to 299	Na–K and Na–K–Ca
Batu Kapur	F	180 to 278	Si parent and Na–K
Pakenjeng	F	<100	Si
Cilayu	F	125 to 177	Na–K
Cikundul	F	111	Na–K
Cisolok	F	139 to 143	Na–K
Parangtritis	F	88	Na–K

V = volcano-hosted, F = fault-hosted.

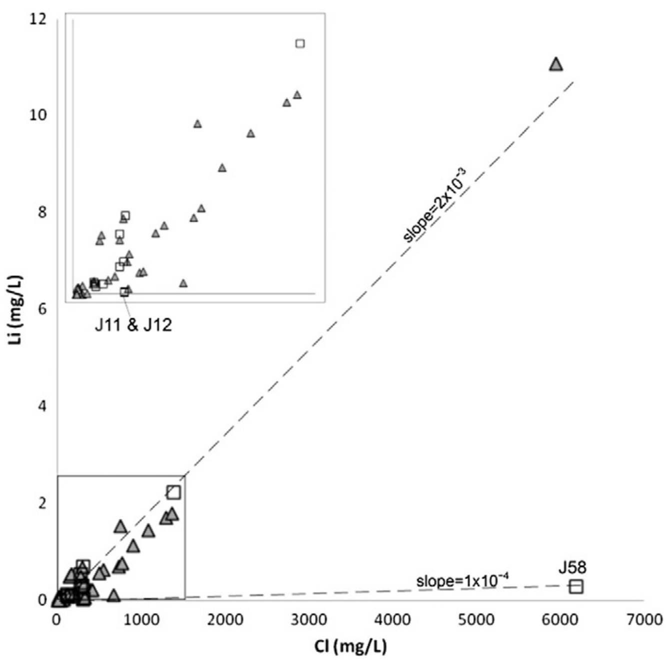

Fig. 8. Li vs. Cl diagram of volcano-hosted and fault-hosted hot springs. Most of the fault-hosted hot springs had similar trends of Li enrichment to those of volcano-hosted hot springs. (Symbols are as in Fig. 3.)

springs (Fig. 8). The slopes of Li enrichment of the volcano-hosted hot springs are ~0.003, but ~0.003 and ~0.0001 for the fault-hosted hot springs. The similarity of high Li enrichment between the fault-hosted and volcano-hosted geothermal fields could be an indication of the same type of heat source, i.e., magmatic. Nevertheless, this assumption has to be corroborated, because the trace element enrichment in hot springs can be generated by several other processes, i.e., (1) high trace element concentration of the host rock, (2) intermediate age and (3) high temperature of the geothermal system (Arehart et al., 2003). The first point was ruled out, because the geothermal host rocks on Java are basically identical, i.e., andesitic rocks. However, the second and the third points were evaluated by considering the calculated reservoir temperatures. The similarity of the high Li enrichment trend and the similarity high reservoir temperatures of fault-hosted and volcano-hosted geothermal systems was considered an indication of a magmatic heat source for both. Meanwhile, an intermediate age of a fault-hosted geothermal system can be concluded when its reservoir temperature is lower than that of a volcano-hosted geothermal system and its Li enrichment is as high as that of a volcano-hosted geothermal system. An intermediate age geothermal system has a relatively higher trace element concentration due to the extended period of water–rock interaction. Young geothermal systems have less time of water–rock interaction and old geothermal systems have already leached most trace elements from their host rocks, thus both systems have relatively low trace element concentrations (Arehart et al., 2003). Considering those assumptions, the fault-hosted geothermal systems of Cilayu, Batu Kapur, Maribaya and Cisolok should be heated by a magmatic heat source. In contrast, such heat source was not likely for the Cikundul and Pakenjeng fault-hosted geothermal systems. Hence, the high Li enrichment of these two fault-hosted geothermal systems was caused by their intermediate age.

All of the low temperature and Li-poor fault-hosted geothermal systems, Cikundul, Pakenjeng, Parangtritis and Pacitan, are located in the southern part of Java island. This area consists of the Tertiary volcanic belt, where volcanism ceased in the last Paleogene. The volcanism then shifted northward forming the Neogene and Quaternary volcanic belts in the central part of the island (Soeria-Atmadja et al., 1994). Under those geological conditions, the heat source of those fault-hosted geothermal systems was likely similar to that described as 'amagmatic' heat source in the Great Basin (USA) and Western Turkey (Faulds et al., 2010). An 'amagmatic' heat source is a deep seated magma, which remains after volcanism has ceased. The name was used to distinguish this heat source from the shallow magmatic heat sources of the Quaternary. As indicated by the exposure of the Cretaceous basement, the southern part of Java island underwent uplift and erosion due to the subduction of the Indo-Australian and Eurasian plates (Clements et al., 2009). As a result the crust became thinner, which in turn increased the heat gradient, causing thermal circulation of groundwater along faults, thus generating the fault-hosted geothermal systems. The same heating mechanism was suggested for geothermal systems along the Alpine fault, New Zealand (Allis and Shi, 1995; Shi et al., 1996).

5.4. Oxygen and hydrogen isotope considerations

The deuterium and oxygen isotopic composition of hot springs can be used to investigate their origin (Craig et al., 1956; Craig, 1963; Arnason, 1977; Giggenbach, 1978; Giggenbach et al., 1983; McCarthy et al., 2005; Pichler, 2005; Majumdar et al., 2009). All of the fault-hosted hot springs and most of the volcano-hosted hot springs plotted close to the Local Meteoric Water Line (LMWL), indicating meteoric water as the source of the hydrothermal fluids (Fig. 9).

Ten volcano-hosted geothermal waters, J9, J10, J19, J24, J26, J32, J51, J59 and J65, show stable isotope enrichment. This could have been caused by either evaporation, water-rock interaction, the input of magmatic fluids input or any combination of the above (Craig, 1966; Giggenbach and Stewart, 1982; D'Amore and Bolognesi, 1994; Ohba et al., 2000; Varekamp and Kreulen, 2000). Using the formulas from Gonfiantini (1986) and Varekamp and Kreulen (2000), a theoretical evaporation line was calculated for 90 °C lake temperature, 22 °C ambient temperature, 80% atmosphere humidity and a $\delta^{18}O$ of −6.9‰ and $\delta^{2}H$ of −45‰ for meteoric water. Samples J10, J26, J32 and J65 plotted close to the evaporation line although only J10, J32 and J65 were affected by evaporation, while the stable isotope enrichment in J26 was likely caused by addition of andesitic water of Taran et al. (1989) and Giggenbach (1992).

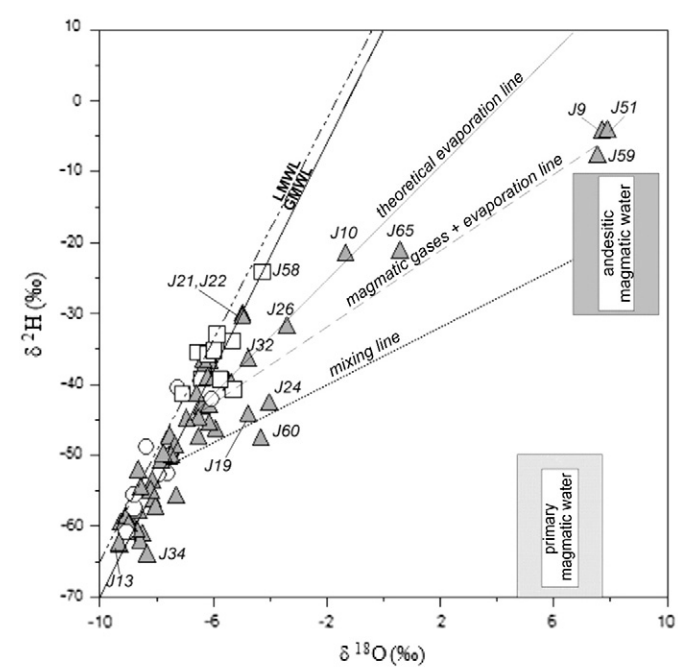

Fig. 9. $\delta^{2}H$ and $\delta^{18}O$ compositions of cold and hot springs. LMWL and GMWL were taken from (Wandowo et al., 2001) and (Craig, 1961), respectively. All of the fault-hosted and most of the volcano-hosted hot springs had a meteoric water origin. Three stable isotope enrichments were identified, i.e., evaporation, combination of magmatic gas input with evaporation and andesitic water input. (Symbols are as in Fig. 3.)

The hot acid crater lakes of Kawah Kamojang (J9), Kawah Putih (J51) and Kawah Sikidang (J59) have the heaviest isotope composition and plotted above the field of andesitic water (Fig. 9). Connecting the hot crater lakes with their respective meteoric water ($\delta^{18}O = -6.9‰$ and $\delta^2H = -45‰$) generates a line, which is flatter than the evaporation line (Fig. 9). The slope of this line is close to the slope of other hot acid crater lakes, such as Khusatsu-Shirane volcano (Ohba et al., 2000), Poas volcano (Rowe, 1994), Kelimutu (Varekamp and Kreulen, 2000) and Kawah Ijen (Delmelle et al., 2000). Thus, the isotopic composition indicated that the hot crater lake fluids likely underwent substantial evaporation and some reaction with magmatic gas.

The presence of andesitic water in the geothermal systems was indicated for samples J19 (Candi Songgoriti 2), J24 (Banyuasin) and J60 (Kawah Sileri), which plot on or near the mixing line between local groundwater and andesitic water (Fig. 9). However, Fig. 10 indicates only andesitic water input for J19, J24 and J26, but not for J60. The plot of J26 on the theoretical evaporation line in Fig. 9 is caused by its lighter stable isotope composition compared to the other hot springs with andesitic water mixing. Andesitic water input was also found, for example, for the Meager Creek (Clark et al., 1982), Larderello (D'Amore and Bolognesi, 1994), Geyser (D'Amore and Bolognesi, 1994), Tongonan (Gerardo et al., 1993), El Chicon volcano (Taran et al., 2008) and Tutum Bay (Pichler et al., 1999) geothermal systems (Fig. 10). In addition, the elevated Cl− concentration in samples J19, J24 and J26 corroborate the presence of andesitic water in those geothermal systems. In contrast to these three samples, the presence of andesitic water could not be confirmed for sample J60, due to its low Cl− concentration. Hence, similar to the J10, J32 and J65 hot springs, stable isotope enrichment of J60 should have been caused by evaporation. The fact that J60 plots below the evaporation is likely due to a lighter stable isotope composition of its meteoric source water compared to that of the meteoric source water, which was used for the calculation of the theoretical evaporation line.

6. Conclusions

Based on the geological setting, two types of geothermal systems were identified on Java, volcano-hosted and fault-hosted. Contribution of CO_2 to the geothermal fluid in a volcano-hosted geothermal system, which was absent/minor in a fault-hosted geothermal system, led to a different water chemistry. Volcano-hosted hot springs had higher $HCO_3{}_-$ concentration and a higher Mg^{2+}/Na^+ ratio than fault-hosted host springs. While the B concentration of fault-hosted hot springs was affected only by water–rock interaction, volcano-hosted hot springs were influenced by phase separation, water–rock interaction and groundwater mixing. Seawater addition was identified in the Parangtritis, which was considered a fault-hosted geothermal system. Calculated reservoir temperatures of volcano-hosted geothermal systems ranged from 125 to 338 °C and those of fault-hosted geothermal systems ranged from 74 to 299 °C.

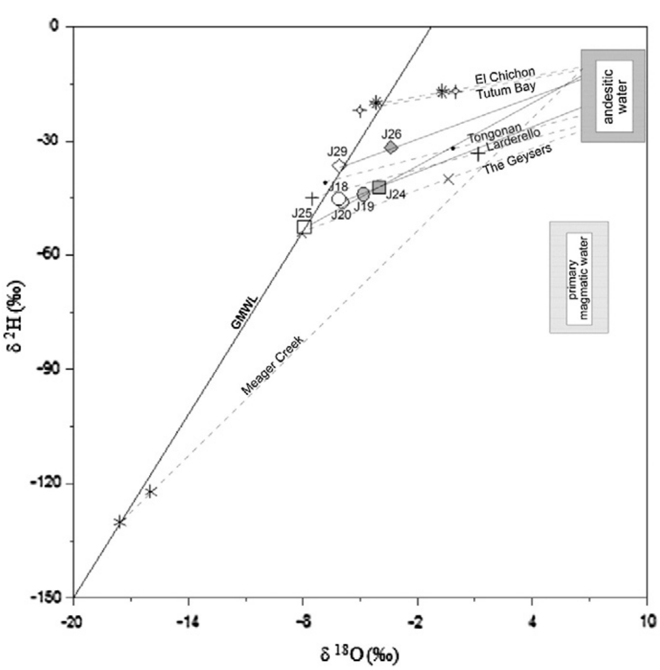

Fig. 10. δ^2H and $\delta^{18}O$ correlation lines between hot springs (gray filled) and their associated cold springs (open) from Java. The dashed lines are stable isotope correlations between thermal waters and their respective meteoric waters from other locations around the world.

Several geothermal systems on Java, although fault-hosted are likely heated by shallow magmas, i.e., Batu Kapur, Maribaya, Cilayu and Cisolok. The addition of volcanic fluids in Batu Kapur and Maribaya, which are located in the active Quarternary volcanic belt, indicated that these two geothermal systems in fact are volcano-hosted geothermal systems. Those fault-hosted geothermal fields that were located in the old (Neogene) volcanic belt did not experience any addition of volcanic fluids. Shallow magma heat sources were not indicated in fault-hosted geothermal systems of Cikundul, Pakenjeng, Pacitan and Parangtritis. Thus, deep seated magma heat sources were suggested for those four geothermal systems.

Stable isotope enrichments were found in ten of the volcano-hosted geothermal systems, but not in any of the fault-hosted geothermal systems. Stable isotope enrichment due to evaporation was recognized in the Kawah Candradimuka and Kawah Sileri, Kawah Hujan and Candi Gedong Songo geothermal systems. A combination of intensive evaporation and magmatic gas input produced very heavy stable isotopes in the hot acid crater lakes of the Kawah Kamojang, Kawah Sikidang and Kawah Putih geothermal systems. The addition of substantial amounts of Andesitic water to the geothermal fluid was observed in the Candi Songgoriti, Banyuasin and Pablengan geothermal systems.

Those findings reject the general assumption of a low energy potential of fault-hosted geothermal systems, since although fault-hosted their heat source can be magmatic as seen for several of the fault-hosted geothermal systems on Java. This should give a new perspective for geothermal exploration on Java, where to date, fault-hosted geothermal systems were excluded from the geothermal energy development program.

Acknowledgments

A part of this study was supported by the Ministry of Energy and Mineral Resources of Indonesia in the form of PhD scholarship grants number: 2579 K/69/MEM/2010. Thanks to Seto and Maman for their help in the sampling campaign. TP acknowledges funding from the German Research Foundation (DFG). M. Rowe and two anonymous reviewers are thanked for their fruitful input and comments on the first version of this manuscript.

Supplementary data

Supplementary data associated with this article can be found in the online version, at http://dx.doi.org/10.1016/j.jvolgeores.2014.08.004. These data include Google maps of the most important areas described in this article.

References

Abrenica, A.B., Harijoko, A., Kusumah, Y.I., Boogie, I., 2010. Characteristics of hydrothermal alteration in part of the northern vapor-dominated reservoir of the Wayang Windu geothermal field, West Java. Proceedings World Geothermal Congress (Bali, Indonesia).

Alam, M.A., Sanchez, P., Parada, M.A., 2010. Interplay of volcanism and structural control in defining the geothermal system(s) along the Liquine-Ofqui fault zone, in the south-central Chile. GRC Trans. 34, 747–750.

Allen, E.T., Day, A.L., 1927. Steam wells and other thermal activity at the Geysers, California. Carnegie Inst Wash Publ 378, 1–106.

Allis, R.G., Shi, Y., 1995. New insights to temperature and pressure beneath the central Southern Alps, New Zealand. N Z J Geol Geophys 38, 585–592.

Alzwar, M., Akbar, N., Bachri, S., 1992. Geological Map of the Garut and Pamengpeuk Quadrangle, Java. Geological Research and Development Centre of Indonesia, Bandung.
Arehart, G.B., Coolbaugh, M.F., Poulson, S.R., 2003. Evidence for a magmatic source of heat for the Steamboat springs geothermal system using trace elements and gas geochemistry. GRC Trans 27, 269–274.
Arnason, B., 1977. Hydrothermal systems in Iceland traced by deuterium. Geothermics 5, 125–151.
Arnorsson, S., Andresdottir, A., 1995. Processes controlling the distribution of boron and chlorine in natural waters in Iceland. Geochim Cosmochim Acta 59, 4125–4146.
Bahar, I., Girod, M., 1983. Controle structural du volcanisme Indonesien (Sumatra, Java-Bali): application et critique de la methode de Nakamura. Bull Soc Geol Fr 7, 609–614.
Chang, C.L., 1984. Triangular diagrams for predication of aquifer chemistry. Geotherm Res Counc Trans 8, 373–376.
Clark, I.D., Fritz, P., Michel, F.A., Souther, J.G., 1982. Isotope hydrogeology and geothermometry of the Mount Meager geothermal area. Can J Earth Sci 19, 1454–1473.
Clements, B., Hall, R., Smyth, H.R., Cottam, M.A., 2009. Thrusting of a volcanic arc: a new structural model for Java. Pet Geosci 15, 159–174.
Craig, H., 1961. Isotopic variations in meteoric waters. Science 133, 1702–1703.
Craig, H., 1963. The isotopic geochemistry of water and carbon in geothermal areas. In: Tongiorgi, E. (Ed.), Nuclear Geology on Geothermal Areas. Consiglio Nazional delle Ricerche, Pisa, pp. 17–53.
Craig, H., 1966. Isotopic composition and origin of the Red Sea and Salton Sea geothermal brines. Science 154, 1544–1548.
Craig, H., Boato, G., White, D.E., 1956. Isotopic geochemistry of thermal waters. National Academic Sciences. National Research Council Publication. 400, pp. 29–38.
D'Amore, F., Bolognesi, L., 1994. Isotopic evidence for a magmatic contribution to fluids of the geothermal systems of Larderello, Italy, and the Geysers, California. Geothermics 23, 21–32.
Delmelle, P., Bernard, A., 1994. Geochemistry, mineralogy, and chemical modeling of the acid crater lake of Kawah Ijen Volcano, Indonesia. Geochim Cosmochim Acta 58, 2445–2460.
Delmelle, P., Bernard, A., Kusakabe, M., Fischer, T.P., Takano, B., 2000. Geochemistry of the magmatic–hydrothermal system of Kawah Ijen volcano, East Java, Indonesia. J Volcanol Geotherm Res 97, 31–53.
Effendi, A.C., Kusnama, Hermanto, B., 1998. Geological Map of the Bogor Quadrangle, Java. Geological Research and Development Centre of Indonesia, Bandung.
Ellis, A.J., Mahon, W.A.J., 1977. Chemistry and Geothermal Systems. Academic Press, New York, (392 pp.).
Faulds, J., Coolbaugh, M., Bouchot, V., Moeck, I., Oğuz, K., 2010. Characterizing structural controls of geothermal reservoirs in the Great Basin, USA, and Western Turkey: developing successful exploration strategies in extended terranes. Proceedings World Geothermal Congress (Bali, Indonesia).
Fournier, R.O., 1977. Chemical geothermometers and mixing models for geothermal systems. Geothermics 5, 41–50.
Fournier, R.O., 1989. Lectures on geochemical interpretation of hydrothermal waters. UNU Geothermal Training Programme, Reykjavik, Iceland, Report 10 (73 pp.).
Gerardo, J.Y., Nuti, S., D'Amore, F., Seastres, J.R., J.S., Gonfiantini, R., 1993. Isotopic evidence for magmatic and meteoric water recharge and the processes affecting reservoir fluids in the Palinpinon geothermal systems, Philippines. Geothermics 22, 521–533.
Giggenbach, W.F., 1978. The isotopic composition of waters from the El Tatio geothermal field, northern Chile. Geochim Cosmochim Acta 42, 979–988.
Giggenbach, W.F., 1984. Mass transfer in hydrothermal systems — a conceptual approach. Geochim Cosmochim Acta 48, 2693–2711.
Giggenbach, W.F., 1988. Geothermal solute equilibria. Derivation of Na–K–Mg–Ca geoindicators. Geochim Cosmochim Acta 52, 2749–2765.
Giggenbach, W.F., 1991. Chemical techniques in geothermal exploration. In: D'Amore, F. (Ed.), Application of Geochemistry in Geothermal Reservoir Development. UNITAR/UNDP, Rome, pp. 252–270.
Giggenbach, W.F., 1992. Isotopic shifts in waters from geothermal and volcanic systems along convergent plate boundaries and their origin. Earth Planet Sci Lett 113, 495–510.
Giggenbach, W.F., 1997. The origin and evolution of fluids in magmatic–hydrothermal systems. In: Barnes, H.L. (Ed.), Geochemistry of Hydrothermal Ore Deposits. Wiley, pp. 737–796.
Giggenbach, W.F., Stewart, M.K., 1982. Processes controlling the isotopic composition of steam and water discharges from steam vents and steam-heated pools in geothermal areas. Geothermics 11, 71–80.
Giggenbach, W.F., Gonfiantini, R., Jangi, B.L., Truesdell, A.H., 1983. Isotopic and chemical composition of Parbati valley geothermal discharges, NW-Himalaya, India. Geothermics 12, 199–222.
Goff, F., Janik, C.J., 2000. Geothermal systems. In: Sigurdsson, H. (Ed.), Encyclopedia of Volcanoes. Academic Press, pp. 817–834.
Gonfiantini, R., 1986. Environmental isotopes in lake studies. In: Frits, P., Fontes, J.C.H. (Eds.), Handbook of Environmental Isotope Geochemistry. Elsevier, Amsterdam, pp. 113–168.
HACH, 2007. Alkalinity Titrator Manual.
Hadi, J., 1997. A hydrothermal alteration study to assess temperature and overprinting from the S-1 exploration well, north Darajat field, Indonesia. Diploma Project Report. Geothermal Institute, The University of Auckland.
Hall, R., 2002. Cenozoic geological and plate tectonic evolution of SE Asia and the SW Pacific: computer-based reconstructions, model and animations. J Asian Earth Sci 20, 353–431.
Hamilton, W., 1979. Tectonics of the Indonesian Region. USGS Professional Paper. 1078.
Harder, H., 1970. Boron content of sediments as a tool in facies analysis. Sediment Geol 4, 153–175.
Hedenquist, J.W., 1990. The thermal and geochemical structure of the Broadlands–Ohaaki geothermal system, New Zealand. Geothermics 19, 151–185.
Henley, R.W., Ellis, A.J., 1983. Geothermal systems ancient and modern: a geochemical review. Earth Sci Rev 19, 1–50.
Hoffmann-Rothe, A., Ritter, O., Haak, V., 2001. Magnetotelluric and geomagnetic modelling reveals zones of very high electrical conductivity in the upper crust of Central Java. Phys Earth Planet In 124, 131–151.
Italiano, F., Bonfanti, P., Pizzino, L., Quattrocchi, F., 2010. Geochemistry of fluids discharged over the seismic area of the Southern Apennines (Calabria region, Southern Italy): implications for fluid–fault relationships. Appl Geochem 25 (4), 540–554.
Kaasalainen, H., Stefánsson, A., 2012. The chemistry of trace elements in surface geothermal waters and steam, Iceland. Chem Geol 330–331, 60–85.
Kuhn, M., 2004. Reactive Flow Modeling of Hydrothermal Systems. Springer-Verlag, Berlin Heidelberg, (261 pp.).
Layman, E.B., Soemarinda, S., 2003. The Patuha vapor-dominated resource West Java, Indonesia. Proceedings 28th Workshop Geothermal Reservoir Engineering (Stanford University, California).
Majumdar, N., Mukherjee, A.L., Majumdar, R.K., 2009. Mixing hydrology and chemical equlibria in Bakreswar geothermal area, Eastern India. J Volcanol Geotherm Res 183, 201–212.
McCarthy, K.T., Pichler, T., Price, R.E., 2005. Geochemistry of Champagne Hot Springs shallow hydrothermal vent field and associated sediments, Dominica, Lesser Antilles. Chem Geol 224 (1–3), 55–68.
Nicholson, K., 1993. Geothermal Fluids: Chemistry and Exploration Techniques. Springer Verlag, (266 pp.).
Ohba, T., Hirabayashi, J., Nogami, K., 2000. D/H and 18O/16O ratios of water in the crater lake at Kusatsu-Shirane volcano, Japan. J Volcanol Geotherm Res 97, 329–346.
Pichler, T., 2005. Stable and radiogenic isotopes as tracers for the origin, mixing and subsurface history of fluids in submarine shallow-water hydrothermal systems. J Volcanol Geotherm Res 139, 211–226.
Pichler, T., Veizer, J., Hall, G.E.M., 1999. The chemical composition of shallow-water hydrothermal fluids in Tutum Bay, Ambitle island, Papua New Guinea and their effect on ambient seawater. Mar Chem 64, 229–252.
Prasetio, R., Abidin, Z., Yulizar, Y., 2010. Isotope and gas geochemistry of Dieng geothermal field, Indonesia. Proceedings World Geothermal Congress (Bali, Indonesia).
Rowe Jr., G.L., 1994. Oxygen, hydrogen, and sulfur isotope systematics of the crater lake system of Poas Volcano, Costa Rica. Geochem J 28, 263–287.
Samodra, H., Gafoer, S., Tjokrosapoetro, S., 1992. Geological Map of the Pacitan Quadrangle, Java. Geological Research and Development Centre of Indonesia, Bandung.
Sarsito, D.A., Meilano, I., Abidin, H.Z., Kato, T., 2011. Five years geodetic GPS observation in the West Java of Java Island. Japan Geoscience Union Meeting.
Satyana, A.H., 2007. Central Java, Indonesia — a 'terra incognita' in petroleum exploration: new considerations on the tectonic evolution and petroleum implications. Proceedings Indonesian Petroleum Association.
Setijadji, L.D., 2010. Segmented volcanic arc and its association with geothermal fields in Java island, Indonesia. Proceedings World Geothermal Congress.
Shi, Y., Allis, R.G., Davey, F., 1996. Thermal modeling of the Southern Alps, New Zealand. Pure Appl Geophys 146, 469–501.
Silitonga, P.H., 1973. Geological Map of the Bandung Quadrangle, Java. Geological Research and Development Centre of Indonesia, Bandung.
Simandjuntak, T.O., Barber, A.J., 1996. Contrasting tectonic styles in the Neogene orogenic belts of Indonesia. Geol Soc Lond Spec Publ 106, 185–201.
Soeria-Atmadja, R., Maury, R.C., Bellon, H., Pringgoprawiro, H., Polve, M., Priadi, B., 1994. Tertiary magmatic belts in Java. J SE Asian Earth Sci 9, 13–27.
Sriwana, T., van Bergen, M.J., Varekamp, J.C., Sumarti, S., Takano, B., van Os, B.J.H., Leng, M.J., 2000. Geochemistry of the acid Kawah Putih lake, Patuha Volcano, West Java, Indonesia. J Volcanol Geotherm Res 97, 77–104.
Sudarman, S., Boedihardi, M., Pudyastuti, K., Bardan, 1995. Kamojang geothermal field: 10 year operation experience. Proceedings of the World Geothermal Congress. 3, pp. 1773–1777 (Florence, Italy).
Sujatmiko, Santosa, S., 1992. Geological Map of the Leuwidamar Quadrangle, Java. Geological Research and Development Centre of Indonesia, Bandung.
Taran, Y.A., Pokrovsky, B.G., Esikov, A.D., 1989. Deuterium and oxygen-18 in fumarolic steam and amphiboles from some Kamchatka volcanoes: 'andesitic waters'. Dokl Akad Nauk SSSR 304, 440–443.
Taran, Y., Rouwet, D., Inguaggiato, S., Aiuppa, A., 2008. Major and trace element geochemistry of neutral and acidic thermal springs at El Chichón volcano, Mexico. J Volcanol Geotherm Res 178 (2), 224–236.
Trompetter, W.J., Reyes, A.G., Vickridge, I.C., Markwitz, A., 1999. Lithium and boron distributions in geological samples. Nucl Inst Methods Phys Res 158, 568–574.
Truesdell, A.H., Haizlip, J.R., Armannsson, H., D'Amore, F., 1989. Origin and transport of chloride in superheated geothermal steam. Geothermics 18, 295–304.
Valentino, G.M., Stanzione, D., 2003. Source processes of the thermal waters from the Phlegraean Fields (Naples, Italy) by means of the study of selected minor and trace elements distribution. Chem Geol 194 (4), 245–274.
Van Bemellen, R.W., 1949. The Geology of Indonesia. vol. 1A. Martinus Nijhoff, the Hague, (732 pp.).
Varekamp, J.C., Kreulen, R., 2000. The stable isotope geochemistry of volcanic lakes, with examples from Indonesia. J Volcanol Geotherm Res 97, 309–327.
Wandowo, Abidin, Z., Alip, Djiono, 2001. Daerah resapan air tanah Cekungan Jakarta. Risalah Pertemuan Ilmiah Penelitian dan Pengambangan Aplikasi Isotop dan Radiasi.
White, D.E., 1957. Thermal waters of volcanic origin. Bull Geol Soc Am 68, 1637–1658.
White, D.E., Muffler, L.P.J., Truesdell, A.H., 1971. Vapour-dominated hydrothermal systems compared with hot-water systems. Econ Geol 66, 75–97.
Wisian, K.W., Blackwell, D.D., Richards, M., 1999. Heat flow in the western United States and extensional geothermal systems. Proceedings 24th Workshop on Geothermal Reservoir Engineering Stanford University.